Inorganic Chemistry

Article

pubs.acs.org/IC

New Fluoride Carbonates: Centrosymmetric $KPb_2(CO_3)_2F$ and Noncentrosymmetric $K_{2.70}Pb_{5.15}(CO_3)_5F_3$

T. Thao Tran and P. Shiv Halasyamani*

Department of Chemistry, University of Houston, 136 Fleming Building, Houston, Texas 77204-5003, United States

Supporting Information

ABSTRACT: Two new potassium lead fluoride carbonates, $KPb_2(CO_3)_2F$ and $K_{2.70}Pb_{5.15}(CO_3)_5F_3$, have been synthesized and characterized. The materials were synthesized through solvothermal and conventional solid-state techniques. $KPb_2(CO_3)_2F$ and $K_{2.70}Pb_{5.15}(CO_3)_5F_3$ were structurally characterized by single crystal X-ray diffraction and exhibit two-dimensional crystal structures consisting of corner-shared PbO_6F and PbO_6F_2 polyhedra. $K_{2.70}Pb_{5.15}(CO_3)_5F_3$ is noncentrosymmetric, and crystallizes in the *achiral* and *nonpolar* space group $P\bar{6}m2$ (crystal class −6m2). Powder second-harmonic generation (SHG) measurements using 1064 nm radiation revealed a SHG efficiency of approximately 40 × α-SiO_2, whereas a charge constant, d_{33}, of approximately 20 pm/V was obtained through converse piezoelectric measurements. For the reported materials, infrared, UV−vis, thermogravimetric, and differential thermal analysis measurements were performed.

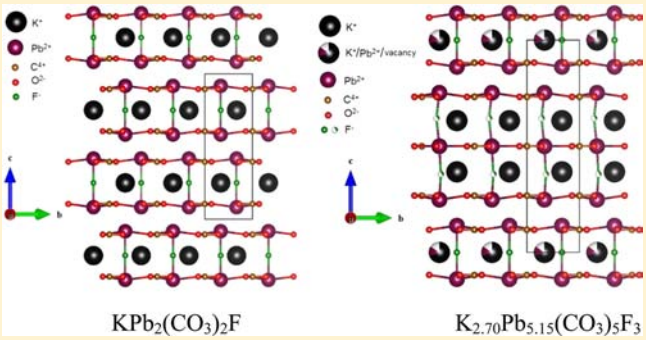

INTRODUCTION

Noncentrosymmetric (NCS) polar compounds have been of significant interest attributable to their technologically important properties such as ferroelectricity and pyroelectricity.[1−4] Other interesting functional properties of NCS but not necessarily polar structures are second-harmonic generation (SHG) and piezoelectricity.[5−8] A number of approaches to the design and synthesis of new NCS materials have been reported.[9−33] We have focused on designing new NCS materials[34−45] by using cations susceptible to second-order Jahn−Teller (SOJT) distortions: octahedrally coordinated d^0 transition-metal cations and lone-pair cations.[46−50] Both families of cations are in asymmetric and locally polar coordination environments attributable to SOJT effects. With lone-pair cations such as Pb^{2+}, Te^{4+}, I^{5+}, and so forth, a stereoactive lone-pair is observed that "pushes" the ligands toward one side of the cation, resulting in a highly asymmetric coordination environment. With respect to contribution of anions to NCS structure, fluoride carbonates have attracted considerable attention over the past 10 years as a result of the polarizability of the carbonate groups.[51−59] The polarizability of anisotropic carbonate group with a π-conjugated system is approximately 5 times greater than that of isotropic fluoride ion.[60,61] The difference in polarizability between these two anions could give rise to the formation of a macroscopically polar material.

A few NCS fluoride carbonates have been reported.[51,62] SHG has been observed in $K_4Ln_2(CO_3)_3F_4$ (where Ln = Nd, Sm, Eu and Gd),[62] with the largest efficiency reported for $K_4Eu_2(CO_3)_3F_4$. In addition, a family of NCS alkaline−alkaline-earth fluoride carbonates, $KSrCO_3F$, $RbSrCO_3F$, $KCaCO_3F$, $RbCaCO_3F$, $CsCaCO_3F$, and $Cs_3Ba_4(CO_3)_3F_5$ were reported recently.[51,58] Of these materials, only $Cs_3Ba_4(CO_3)_3F_5$ is polar, whereas the others are nonpolar and achiral. These materials have a wide transparency in the UV, in the range of 200−800 nm, except for $Cs_3Ba_4(CO_3)_3F_5$ with a UV cutoff at approximately 210 nm. The alkaline−alkaline-earth fluoride carbonates are SHG active with efficiencies of 1−3 × KDP (40−120 × α-SiO_2). Finally, transition metal fluoride carbonates, $KCuCO_3F$,[63] $BaMCO_3F_2$ (where M = Mn, Cu and Zn),[56,64] and $Ba_2Co(CO_3)_2F_2$[54] have also been reported. Of these materials, only $KCuCO_3F$ is NCS and polar, whereas the others are centrosymmetric. No SHG, piezoelectric, or polarization properties have been reported for $KCuCO_3F$.

We have been interested in investigating the association of a lone-pair cation, Pb^{2+}, and carbonate fluoride anions to couple their acentric features and thereby enhance the formation of a new NCS material. To date, no material in the A^+−Pb^{2+}−CO_3^{2-}−F^- system (where A^+ = Li^+, Na^+, K^+, Rb^+, or Cs^+) has been reported. Our investigation of the K−Pb−CO_3−F system resulted in two new potassium lead fluoride carbonates, $KPb_2(CO_3)_2F$ and $K_{2.70}Pb_{5.15}(CO_3)_5F_3$. $K_{2.70}Pb_{5.15}(CO_3)_5F_3$ is NCS and crystallizes in *achiral* and *nonpolar* space group $P\bar{6}m2$. In this paper, we report the synthesis, structure, characterization, and structure-property relationships of both materials.

Received: October 29, 2012
Published: February 8, 2013

In addition, for $K_{2.70}Pb_{5.15}(CO_3)_5F_3$ we investigate its functional properties: SHG and piezoelectricity.

■ EXPERIMENTAL SECTION

Reagents. KF (Alfa Aesar, 99.5%), $Pb(OAc)_2.3H_2O$, PbF_2, $PbCO_3$ (Sigma-Aldrich, 99.9%), MeOH (Sigma-Aldrich, 99%), and CF_3COOH (Sigma-Aldrich, 99%) were used as starting materials.

Synthesis. Crystals of $KPb_2(CO_3)_2F$ and $K_{2.70}Pb_{5.15}(CO_3)_5F_3$ were grown by solvothermal techniques using a mixture of methanol and trifluoroacetic acid as a solvent. The reaction mixture of 0.379 g (1.00 × 10^{-3} mol) of $Pb(OAc)_2{\cdot}3H_2O$, 0.232 g (4.00 × 10^{-3} mol) of KF, 1.50 mL (3.71 × 10^{-2} mol) of methanol, and 1.50 mL (1.94 × 10^{-2} mol) of trifluoroacetic acid were placed in a 23-mL Teflon-lined stainless steel autoclave. The autoclave was closed, gradually heated up to 180 °C, held for 24 h, and then slowly cooled to room temperature at a rate of 6 °C h^{-1}. The solid products were isolated from the mother-liquor by vacuum filtration and washed with ethanol. Colorless hexagonal plate-like crystals and block-shaped crystals, subsequently determined to be $KPb_2(CO_3)_2F$ and $K_{2.70}Pb_{5.15}(CO_3)_5F_3$, respectively, were obtained as a mixture in which the latter is the major phase, approximately 70% (Supporting Information, Figure S1). The reported compounds are slightly hygroscopic; thus the products were stored in a vacuum desiccator.

Polycrystalline $KPb_2(CO_3)_2F$ and $K_{2.70}Pb_{5.15}(CO_3)_5F_3$ were synthesized by conventional solid-state techniques. For $KPb_2(CO_3)_2F$, stoichiometric amounts of KF (0.116 g, 2.00 × 10^{-3} mol) and $PbCO_3$ (1.07 g, 4.00 × 10^{-3} mol) were thoroughly ground and pressed into pellet. The pellet was placed in alumina boat that was heated to 250 °C in flowing CO_2 gas, held for 2 days, and then cooled to room temperature at a programmed rate of 180 °C h^{-1}. For $K_{2.70}Pb_{5.15}(CO_3)_5F_3$, amounts of KF (0.126 g, 2.16 × 10^{-3} mol), $PbCO_3$ (1.07 g, 4.00 × 10^{-3} mol), and PbF_2 (0.029 g, 0.12× 10^{-3} mol) were thoroughly ground and pressed into pellet. The pellet was placed in alumina boat that was heated to 270 °C in flowing CO_2 gas, held for 3 days, and then cooled to room temperature at a programmed rate of 180 °C h^{-1}. The materials were determined to be pure by powder X-ray diffraction (Supporting Information, Figure S1).

Single-Crystal X-ray Diffraction. A colorless hexagonal plate crystal (0.10 × 0.10 × 0.03 mm^3) and a colorless block-shaped crystal (0.10 × 0.10 × 0.05 mm^3) were selected for single-crystal diffraction analysis. Data were collected on a Bruker SMART APEX2 diffractometer equipped with a 4K CCD area detector using graphite-monochromated Mo−Kα radiation. For each sample a hemisphere of data was collected using a narrow-frame method with scan widths of 0.30° in ω. Exposure times were 90 s per frame for $KPb_2(CO_3)_2F$ and 50 s per frame for $K_{2.70}Pb_{5.15}(CO_3)_5F_3$. Both crystals were found to be slightly nonmerohedrally twinned. This minor twinning did not impact the subsequent solution and refinements. Data were integrated using the Bruker SAINT program,[65] with the intensities corrected for Lorentz factor, polarization, air absorption, and absorption attributable to the variation in the path length through the detector faceplate. An empirical absorption correction was made. The positions of the lead atoms were determined by Patterson methods using SHELXS-97,[66] and the remaining atoms were located by difference Fourier maps and least-squares cycles utilizing SHELXL-97.[67] All calculations were performed using WinGX-98 crystallographic software package.[68] Relevant crystallographic data, selected bond distances and angles for $KPb_2(CO_3)_2F$ and $K_{2.70}Pb_{5.15}(CO_3)_5F_3$ are given in Tables 1−2. Atomic coordinates and equivalent isotropic displacement parameters are shown in the Supporting Information, Table S1− S2.

There are some unusual features in the structure of $K_{2.70}Pb_{5.15}(CO_3)_5F_3$. The F(1) atom was found to be disordered about a 3m site. Initially the material was thought to be $K_3Pb_5(CO_3)_5F_3$; however, the anisotropic displacement parameters of the K(2) cation in the double layer consistently refined to a nonpositive definite value. Since K and Pb are the only heavy elements present, it was clear that there had to be a mix of these two elements at this position. Furthermore, since Pb^{2+} has twice the charge of K^+ there had to be a vacancy present for each Pb^{2+} cation to maintain charge balance. When a mixed occupancy model of 70% K^+/15% Pb^{2+}/15% vacancy was placed at the original "K(2)" site, the overall model refined very nicely, resulting in a formula of $K_{2.70}Pb_{5.15}(CO_3)_5F_3$. Changing the amount of Pb present from 5 to 5.15 represents only a 3% increase, which is quite plausible under the reaction conditions. Also, this model results in a Pb:K ratio of 1.9 in $K_{2.70}Pb_{5.15}(CO_3)_5F_3$ that is not very different from the ratio of 2.0 found in the

Table 1. Crystallographic Data

	$KPb_2(CO_3)_2F$	$K_{2.70}Pb_{5.15}(CO_3)_5F_3$
M/g mol^{-1}	592.50	1529.65
T/ K	296(2)	301(2)
λ/ Å	0.71073	0.71073
crystal system	hexagonal	hexagonal
space group	$P6_3/mmc$ (No. 194)	$P\bar{6}m2$ (No. 187)
a/ Å	5.3000(2)	5.3123(5)
b/ Å	5.3000(2)	5.3123(5)
c/ Å	13.9302(8)	18.6203(17)
α/ deg	90	90
β/ deg	90	90
γ/ deg	120	120
V/ $Å^3$	338.88(3)	455.07(7)
Z	2	1
D_c/g cm^{-3}	5.807	5.582
μ/mm^{-1}	50.237	48.194
$2\theta_{max}$/deg	58.48	54.70
R_{int}	0.0471	0.0478
GOF	1.340	1.159
R(F)[a]	0.0187	0.0207
$R_w(F_o^2)$[b]	0.0512	0.0598
Flack parameter	N/A	0.012(18)

[a] $R(F) = \sum||F_o| - |F_c||/\sum|F_o|$. [b] $R_w(F_o^2) = [\sum w(F_o^2 - F_c^2)^2/\sum w(F_o^2]^{1/2}$.

Table 2. Selected Bond Distances (Å) and Angles (deg)

$KPb_2(CO_3)_2F$		$K_{2.70}Pb_{5.15}(CO_3)_5F_3$	
Pb(1)−O(1) × 6	2.6829(6)	Pb(1)−O(1) × 6	2.6668(9)
Pb(1)−F(1)	2.3327(3)	Pb(1)−F(1) × 2	2.454(9)
C(1)−O(1) × 3	1.277(3)	Pb(2)−O(2) ×6	2.6918(11)
		Pb(2)−F(1)	2.254(10)
O(1)−Pb(1)−O(1)	48.68(15)		
O(1)−Pb(1)−O(1)	70.28(15)	Pb(3)−O(3) × 6	2.6926(11)
F(1)−Pb(1)−O(1)	82.86(9)	Pb(3)−F(2)	2.3478(8)
Pb(1)−F(1)−Pb(1)	180.00	C(1)−O(1) × 3	1.296(9)
		C(2)−O(2) × 3	1.293(7)
		C(3)−O(3) × 3	1.282(7)
		O(1)−Pb(1)−O(1)	49.8(4)
		O(1)−Pb(1)−O(1)	70.2(4)
		F(1)−Pb(1)−O(1)	89.55(7)
		F(1)−Pb(1)−F(1)	175.0(7)
		O(2)−Pb(2)−O(2)	49.2(3)
		O(2)−Pb(2)−O(2)	69.6(3)
		F(1)−Pb(2)−O(2)	81.76(15)
		O(3)−Pb(3−O(3)	48.7(3)
		O(3)−Pb(3)−O(3)	70.1(3)
		F(2)−Pb(3)−O(3)	82.25(14)
		Pb(1)−F(1)−Pb(2)	169.5(16)

dx.doi.org/10.1021/ic302357h | Inorg. Chem. 2013, 52, 2466−2473

cocrystallizing material $KPb_2(CO_3)_2F$. For verification purposes we collected data on a second crystal from the same batch, and the results were not significantly different between the two refinements. Both cif's have been deposited in the Supporting Information.

Powder X-ray Diffraction. Powder X-ray diffraction (PXRD) measurements on $KPb_2(CO_3)_2F$ and $K_{2.70}Pb_{5.15}(CO_3)_5F_3$ materials were performed using a PANalytical X'Pert PRO diffractometer equipped with Cu Kα radiation. The data were collected in the 2θ range of 5°−70° with a step size of 0.008° and a scan time of 0.3 s. No impurities were observed, and the experimental and calculated PXRD are in very good agreement (Supporting Information, Figure S1).

Infrared (IR) Spectroscopy. Mid-Infrared (MIR) data were collected in a reflectance mode in an inert atmosphere using an Alpha-P (Bruker Optik) spectrometer (spectral resolution 4 cm^{-1}) built into a glovebox (MBraun) in the 400−4000 cm^{-1} range (Supporting Information, Figure S2).

UV−vis Diffuse Reflectance Spectroscopy. UV−visible reflectance data were collected on a Varian Cary 500 Scan UV−vis−NIR spectrophotometer over the 200−2000 nm spectral range at room temperature. Poly(tetrafluoroethylene) was used as a diffuse reflectance standard. The reflectance spectrum was converted to absorption using the Kubelka−Munk function.[69,70] (Supporting Information, Figure S3).

Thermal Analysis. Thermogravimetric analyses were performed on an EXSTAR TG/DTA 6300 instrument. Approximately 20 mg of $KPb_2(CO_3)_2F$ and $K_{2.70}Pb_{5.15}(CO_3)_5F_3$ were placed separately in a platinum pan and heated at a rate of 10 °C min^{-1} from room temperature to 900 °C under flowing N_2 (Supporting Information, Figure S4).

Second-Harmonic Generation (SHG). Powder SHG measurements were performed on a modified Knurtz-nonlinear optical (NLO) system using a pulsed Nd:YAG laser with a wavelength of 1064 nm. A detailed description of the equipment and methodology has been published.[71] As the powder SHG efficiency has been shown to strongly depend on particle size,[72] $K_{2.70}Pb_{5.15}(CO_3)_5F_3$ was ground and sieved into distinct particle size ranges (<20, 20−45, 45−63, 63−75, 75−90, >90 μm). Relevant comparisons with known SHG materials were made by grinding and sieving crystalline α−SiO_2 and $LiNbO_3$ into the same particle size ranges. No index matching fluid was used in any of the experiments (Supporting Information, Figure S6).

Piezoelectric Measurements. Converse piezoelectric measurements were performed using a Radiant Technologies RT66A piezoelectric test system with a TREK (model 609E-6) high voltage amplifier, Precision Materials Analyzer, Precision High Voltage Interface and MTI 2000 Fotonic Sensor. $K_{2.70}Pb_{5.15}(CO_3)_5F_3$ was pressed into pellets (~1.2 cm diameter, ~0.7 mm thickness) and sintered at 260 °C for 3 days. Silver paste was applied to both sides of the pellet, and the pellet was cured at 250 °C for 12 h (Supporting Information, Figure S7). For all of the structural figures, the program VESTA was used.[73]

Energy-Dispersive X-ray Spectroscopy (EDS) Analysis. A JEOL JSM 6330F scanning electron microscope equipped with an electron dispersive spectrometer was used to determine the lead to potassium ratio. The collected crystal of $K_{2.70}Pb_{5.15}(CO_3)_5F_3$ was mounted on one flat face and coated with 25 nm carbon. Intensity data were processed by Oxford IsisLink software. Standards used were $KAlSi_3O_8$ for potassium, $PbCrO_4$ for lead, CaF_2 for fluorine, and graphite for carbon. Three analyses on this sample were obtained with a focused beam of 15 keV accelerating voltage and 12 μA emission current; one on each of the three visible faces. (Supporting Information, Figure S8).

■ RESULTS AND DISCUSSION

Structures. $KPb_2(CO_3)_2F$ exhibits a two-dimensional crystal structure that consists of double-layers of $Pb(CO_3)_3F$ polyhedra (see Figure 1). The Pb^{2+} cations are connected by carbonate groups in the *ab*-plane, whereas along the *c*-axis direction the connectivity is through a bridging fluoride. The K^+ cations are located in the cavities formed between $Pb(CO_3)_3F$ polyhedral blocks. The double-layers are staggered about the *c*-axis to minimize Pb^{2+} lone-pair−lone-pair interactions. In connectivity terms, the material may be written as $\{2\text{-}[PbO_{6/3}F_{1/2}]^{5/2-}\ 2[CO_{3/3}]^{2+}\}^{-}$, with charge balance maintained by one K^+ cation. Each Pb^{2+} cation is bonded to six oxygen

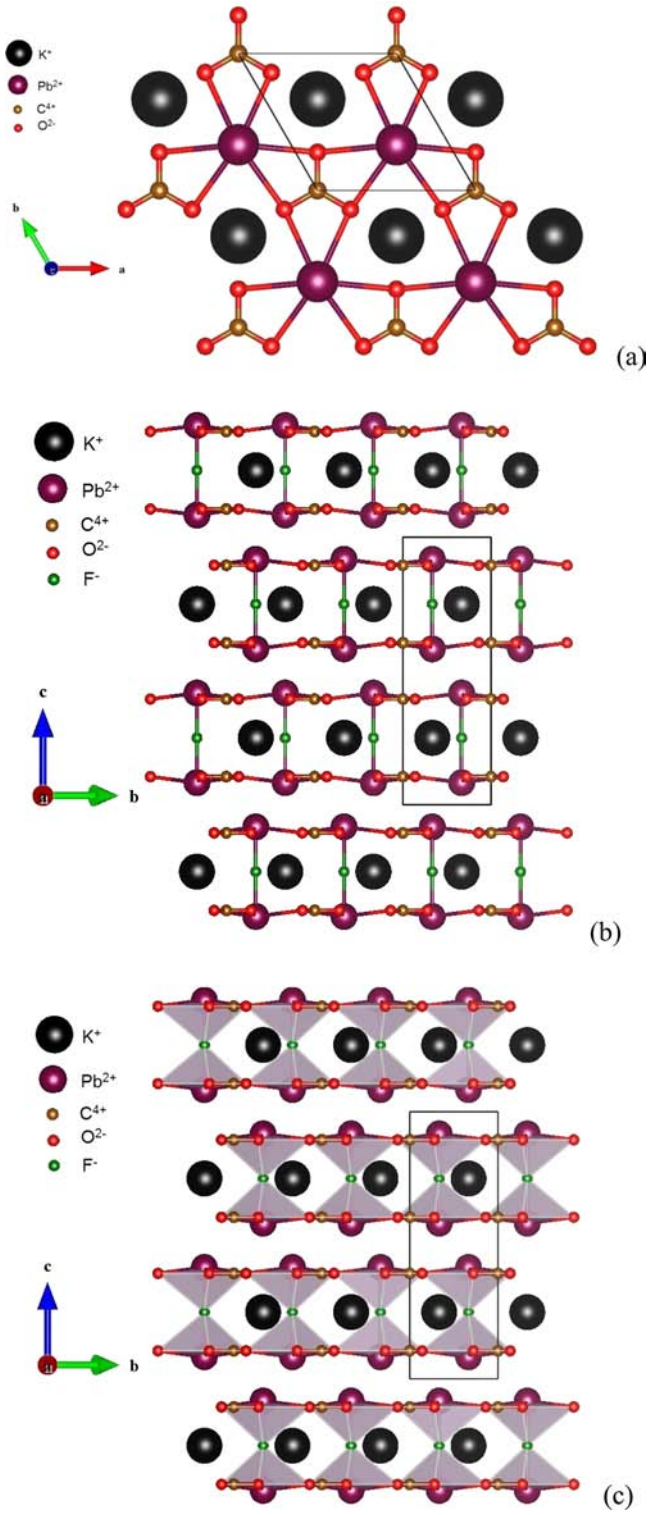

Figure 1. Ball-and-stick representation of a single $Pb(CO_3)$ layer in the *ab*-plane and the K^+ cations beneath this layer (a). Ball-and-stick (b) and polyhedral (c) representations of $KPb_2(CO_3)_2F$ in the *bc*-plane. Note that the double-layers are staggered to minimize lone-pair −lone-pair interactions.

atoms and one fluorine atom in a distorted hexagonal pyramidal coordination environment, with Pb−O distances of 2.6829(6) Å and a Pb−F distance 2.3327(3) Å. The carbonate C−O distance is 1.277(3) Å. The K^+ cation is surrounded by six oxygen atoms with K−O distances of 2.679(4) Å. Bond valence calculations resulted in values of 1.36, 1.72, and 4.05 for K^+, Pb^{2+}, and C^{4+}, respectively (Supporting Information, Table S3).[74,75]

$K_{2.70}Pb_{5.15}(CO_3)_5F_3$ also exhibits a two-dimensional structure that consists of double-layers of $Pb(CO_3)_3F$ polyhedra and triple-layers of $Pb(CO_3)_3F$ and $Pb(CO_3)_3F_2$ polyhedra (see Figure 2). The double-layer alternates with the triple-layer, stacking along the *c* direction. The Pb^{2+} cations are connected by carbonate groups in the *ab*-plane, and along the *c*-axis direction the connectivity is through a bridging fluoride. In the triple-layer, the K^+ cations are located in cavities formed between the $Pb(CO_3)_3F$ and $Pb(CO_3)_3F_2$ polyhedral blocks. In the double-layer the bridging fluoride F(2) is ordered, whereas in the triple layer the bridging fluoride F(1) is statistically disordered with a Pb−F−Pb angle of 169.5(16)°. The $Pb(2)^{2+}$ and $Pb(3)^{2+}$ cations are in distorted hexagonal pyramidal coordination environments with Pb(2)−O(2) (Pb(3)−O(3)) distances of 2.6918(11) Å (2.6926(11) Å), and Pb(2)−F(1) (Pb(3)−F(2)) distances of 2.254(10) Å (2.3478(8) Å). The $Pb(1)^{2+}$ cation is found in a distorted hexagonal bipyramidal environment with Pb(1)−O(1) distances of 2.6668(9) Å and Pb(1)−F(1) distances of 2.454(9) Å. As would be expected, the outer Pb(2)−F(1) distance is considerably shorter than the central Pb(1)−F(1) distance. The K^+ cations are surrounded by six oxygen atoms with K−O distances that range between 2.669(7) Å and 2.858(7) Å. The C−O bond distances range from 1.282(7) to 1.296(9) Å. Bond valence sum calculations resulted in values of 1.01, 1.67−1.97, and 3.87−4.02 for K^+, Pb^{2+}, and C^{4+}, respectively (Supporting Information, Table S4).[74,75]

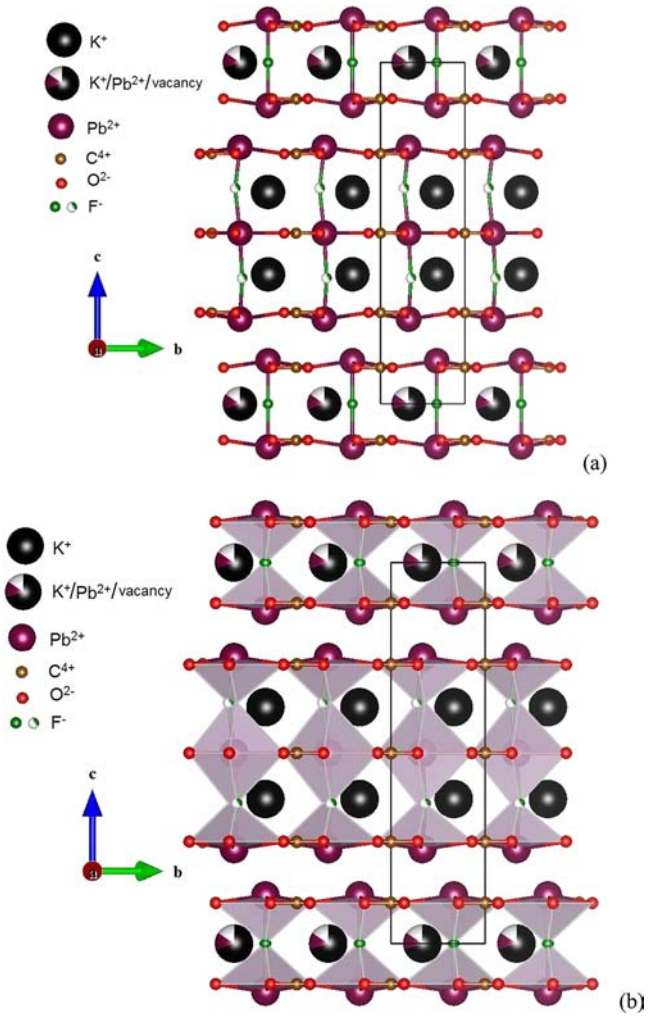

Figure 2. Ball-and-stick (a) and polyhedral (b) representations of $K_{2.70}Pb_{5.15}(CO_3)_5F_3$ in the *bc*-plane. Only one position of the disordered bridging fluoride in the triple layer is shown.

The role of the planar carbonate group with respect to the rest of the structure has been described earlier.[76−78] In fluoride carbonates, the carbonate group may be flat (parallel) or inclined (on-edge) with respect to the overall structure. In both $KPb_2(CO_3)_2F$ and $K_{2.70}Pb_{5.15}(CO_3)_5F_3$, the planar carbonate groups are parallel to the structural layers. This is similar to other reported fluoride carbonates such as $NaBaCe_2(CO_3)_4F$[79] and $BaCe(CO_3)_2F$.[80] Along the *c*-axis, the planar carbonate groups are eclipsed within the double ($KPb_2(CO_3)_2F$) and triple-layer ($K_{2.70}Pb_{5.15}(CO_3)_5F_3$) blocks, but are staggered between blocks. One interesting feature of the outer $Pb(CO_3)F$ layers is that the CO_3 groups are not in the plane of the Pb atoms, but instead are pushed in toward the interior of the layers (see Figure 3). The CO_3 planes are offset by about 0.36 Å from the Pb planes. This is most likely caused by steric repulsion from the lone-pair of electrons on the Pb atoms. The Pb−O distances in the outer $Pb(CO_3)F$ layers are longer than that in the central $Pb(CO_3)F_2$ layers in $K_{2.70}Pb_{5.15}(CO_3)_5F_3$ attributable to the offset position of the CO_3 groups.

In both materials the asymmetric coordination environments of the outer Pb^{2+} atoms of each layer are polar, that is, each PbO_6F polyhedron exhibits a local dipole moment. Since both double-layers and triple-layers are composed of PbO_6F polyhedra with equal and opposite polarizations, the net dipole moments in $KPb_2(CO_3)_2F$ and $K_{2.70}Pb_{5.15}(CO_3)_5F_3$ are zero. Therefore, the structures are macroscopically not polar.

A common feature for $KPb_2(CO_3)_2F$ and $K_{2.70}Pb_{5.15}(CO_3)_5F_3$ is the occurrence of double-layers of PbO_6F polyhedra (see Figure 3a). Although single-layer PbO_6F polyhedra have been previously observed in $BaPb_2(CO_3)_2F_2$,[52,59] the materials in this report are the first examples of double-layer and triple-layer polyhedra composed of PbO_6F and PbO_6F_2 (see Figure 3). Analogous AO_6F_2 (A = Sr^{2+} or Ca^{2+}) polyhedra have been observed previously in $KSrCO_3F$, $RbSrCO_3F$, and $KCaCO_3F$.[51,52] Thus, the central Pb^{2+} cation in the triple-layer may be considered to have an inert rather than stereoactive lone-pair, that is, the lone-pair is more spherical. A stereoactive lone-pair on Pb^{2+} is found in the double-layer in both materials, as well as in the outer PbO_6F polyhedra of the triple-layer. To visualize the lone-pair on the Pb^{2+} cations, ELF calculations were performed on both materials using the VASP package[81,82] with the PBE exchange-correlation functional,[83] and an η = 0.5 (see Figure 4).[73]

Unusual Features of $K_{2.70}Pb_{5.15}(CO_3)_5F_3$. With regard to the nonstoichiometric formula for $K_{2.70}Pb_{5.15}(CO_3)_5F_3$, there is precedence for partial substitution of Pb^{2+} at K^+ sites.[84,85] Pb^{2+} has a six-coordinate effective ionic radius of 1.19 Å, that is only 10% smaller than K^+ (1.38 Å).[83] Thus both cations may occupy the same crystallographic site. Site disorder between Pb^{2+} and K^+ has been reported in KPb_2Cl_5 and $Na_{2-x}K_xPb_{11}F_{18}X_6$ (X =

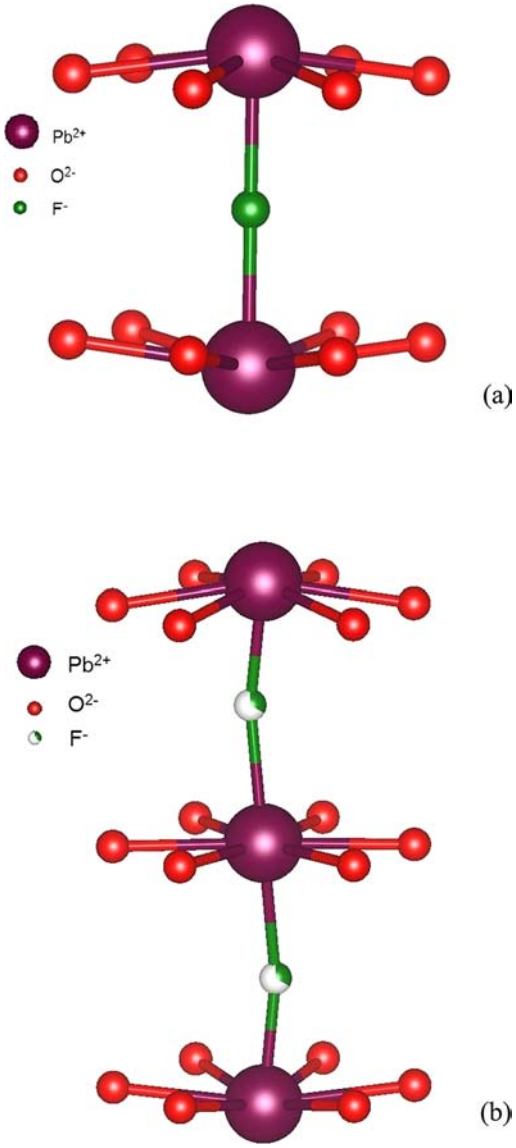

Figure 3. Ball-and-stick representation of (a) the double-layer unit consisting of two PbO_6F distorted hexagonal pyramids and (b) the triple-layer unit consisting of two PbO_6F distorted hexagonal pyramids alternating with one PbO_6F_2 distorted hexagonal bipyramid.

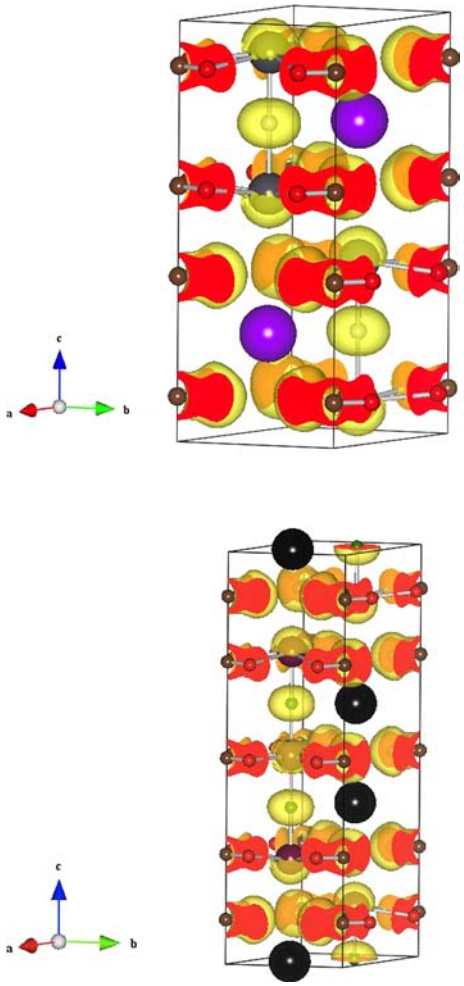

Figure 4. ELF diagram, η = 0.5, of the double-layer in $KPb_2(CO_3)_2F$ (top) and the triple-layer in $K_{2.70}Pb_{5.15}(CO_3)_5F_3$ (bottom). Note that in both materials the "capping" Pb^{2+} cations exhibit a stereoactive lone-pair, whereas the central Pb^{2+} in $K_{2.70}Pb_{5.15}(CO_3)_5F_3$ exhibits an inert lone-pair.

Cl, Br).[84,85] There is also no structural issue with having a partial vacancy at this site since the double-layer skeleton, composed of planes of $Pb(CO_3)$ linked by F, is quite rigid (see Figure 2). The double-layer framework is not perturbed in any significant way by the absence of a cation in the cavities 15% of the time, as evidenced by comparison with the fully occupied double-layer in $KPb_2(CO_3)_2F$. Note that the *a* and *b* unit cell dimensions in both materials are virtually identical (5.3000(2) Å vs 5.3123(5) Å)—a function of the $Pb(CO_3)$ bonding pattern (see Figure 1a)—and the Pb−F distances in the double-layers are also essentially the same (2.3327(3) Å vs 2.3478(8) Å). Although both crystals measured showed the same Pb:K ratio, it should be noted that there is nothing particularly special about the 70% K^+/15% Pb^{2+} composition. It is quite possible that each individual crystal of this material is composed of a different K:Pb ratio, and the crystals we used are simply representative samples.

NCS Considerations. The double-layer units in both $KPb_2(CO_3)_2F$ and $K_{2.70}Pb_{5.15}(CO_3)_5F_3$ are structurally the same, consisting of two nearly planar arrangements of $Pb(CO_3)$ linked by bridging F atoms. The CO_3 groups in each layer are in an eclipsed configuration when viewed down the *c* axis, which is necessitated by the large cations in the cavities between layers. Careful inspection of this eclipsed double-layer structure indicates that it is not possible for this building unit to reside on an inversion center since the F and K atoms have trigonal symmetry in the *ab* plane with respect to each other. Thus it is impossible for an ordered arrangement to have an inversion center at any site in this plane. Similarly the triple-layer unit in $K_{2.70}Pb_{5.15}(CO_3)_5F_3$ cannot possibly reside on an inversion center since the central Pb and C atoms have trigonal symmetry in the *ab* plane. The double and triple-layers that comprise both of these compounds are inherently NCS. Therefore the only way for these materials to pack in a centrosymmetric arrangement is for there to be an inversion center between the individual multilayer sheets. In $KPb_2(CO_3)_2F$ there is an inversion center between each of the double-layers, and the space group is centrosymmetric, $P6_3/mmc$. However there is no way to form an inversion center between the alternating double and triple-layers of

$K_{2.70}Pb_{5.15}(CO_3)_5F_3$, and therefore this material necessarily crystallizes in a NCS space group, $P\bar{6}m2$.

Infrared (IR) Spectroscopy. The IR spectra of $KPb_2(CO_3)_2F$ and $K_{2.70}Pb_{5.15}(CO_3)_5F_3$ revealed C−O vibrations between 1400−680 cm^{-1}. The strong broad bands observed at 1398 and 1400 cm^{-1} can be assigned to the stretching C−O vibrations. The out-of-plane vibration, δ-(OCO), is observed in the range of 850−830 cm^{-1} as a medium band, and the bending vibration, δ(OCO), should appear at 720−680 cm^{-1} as a medium weak band.[86−89] A strong band, however, was observed in the range of 720−680 cm^{-1} which can be attributed to the overlap between the bending vibration, δ(OCO), and the stretching vibration, ν(Pb−O).[88,89] The ν(Pb−F) vibration is observed at ∼400 cm^{-1}.[89] The infrared spectra have been deposited in the Supporting Information, Figure S2.

UV−vis Diffuse Reflectance Spectroscopy. The UV−vis diffuse reflectance spectra revealed that the absorption energies for $KPb_2(CO_3)_2F$ and $K_{2.70}Pb_{5.15}(CO_3)_5F_3$ are approximately 3.9 and 3.8 eV, respectively. This is consistent with the white color of the materials. Absorption (K/S) data were calculated from the Kubelka−Munk function.[69,70]

$$F(R) = \frac{(1-R)^2}{2R} = \frac{K}{S}$$

where R represents the reflectance, K the absorption coefficient, and S the scattering factor. In a K/S versus E (eV) plot, extrapolating the linear part of the rising curve to zero resulted in the onset of absorption at 3.9 and 3.8 eV. The UV−vis diffuse reflectance spectra have been deposited in the Supporting Information, Figure S3.

Thermal Analysis. The thermal behaviors of $KPb_2(CO_3)_2F$ and $K_{2.70}Pb_{5.15}(CO_3)_5F_3$ were investigated using thermogravimetric analysis (TGA) and differential thermal analysis (DTA) under N_2 atmosphere. The decomposition of both materials begins at approximately 290 °C, corresponding to the loss of CO_2. The experimental weight loss is in good agreement with the calculated weight loss. The endothermic peaks in the heating curve are consistent with the decomposition of the materials. The exothermic peaks in the cooling cycle indicate recrystallization of the residues. At approximately 830 °C, weight loss was observed that is likely attributable to the loss of fluorides. Powder XRD data of the residuals revealed PbO and unidentified phases. The DTA/TGA diagrams and powder XRD spectra for $KPb_2(CO_3)_2F$ and $K_{2.70}Pb_{5.15}(CO_3)_5F_3$ have been deposited in the Supporting Information,Figures S4 and S5.

Second-Harmonic Generation (SHG) and Piezoelectric Measurements. Since $K_{2.70}Pb_{5.15}(CO_3)_5F_3$ crystallizes in the NCS space group $P\bar{6}m2$, we investigated the SHG and piezoelectric properties. Powder SHG measurements using 1064 nm radiation revealed a SHG efficiency of approximately 40 × α−SiO_2 in the 45−63 μm particle size range. A relatively weak SHG efficiency is expected as $K_{2.70}Pb_{5.15}(CO_3)_5F_3$ is achiral and nonpolar. Additional SHG measurements, particle size vs SHG efficiency, indicate $K_{2.70}Pb_{5.15}(CO_3)_5F_3$ exhibits type 1 phase-matching behavior. As such $K_{2.70}Pb_{5.15}(CO_3)_5F_3$ falls into the class B category of SHG materials, as defined by Kurtz and Perry (Supporting Information, Figure S6).[64] Based on these measurements, we estimate an average NLO susceptibility, $\langle d_{eff}\rangle_{exp}$, of approximately 7.3 pm/V. Converse piezoelectric measurements were also performed, and a piezoelectric charge constant, d_{33}, of approximately 20 pm/V was determined (Supporting Information, Figure S7).

Energy-Dispersive X-ray Spectroscopy (EDS) Analysis. The semiquantitative EDS measurements were taken three times from the same $K_{2.70}Pb_{5.15}(CO_3)_5F_3$ crystal that was used for X-ray diffraction analysis. The average Pb:K ratio of 1.94(3) found by EDS is in excellent agreement with the value of 1.91 determined by least-squares refinement of the X-ray data. By contrast, if this site were fully occupied by K^+, the Pb:K ratio would be 1.67.

■ CONCLUSIONS

We have synthesized and characterized two new fluoride carbonates, $KPb_2(CO_3)_2F$ and $K_{2.70}Pb_{5.15}(CO_3)_5F_3$. Both materials exhibit two-dimensional layered structures. $KPb_2(CO_3)_2F$ consists of double-layers of $Pb(CO_3)_3F$ polyhedra, whereas $K_{2.70}Pb_{5.15}(CO_3)_5F_3$ consists of double-layers of $Pb(CO_3)_3F$ polyhedra that alternate with triple-layers of $Pb(CO_3)_3F$−$Pb(CO_3)_3F_2$−$Pb(CO_3)_3F$ polyhedra. This results in nearly planar sheets of $Pb(CO_3)$ joined together by bridging fluorides. Both of these double and triple-layer structural units are inherently noncentrosymmetric, since they are composed entirely of elements possessing trigonal symmetry in the *ab* plane. The stacked double-layer units in $KPb_2(CO_3)_2F$ crystallize with inversion centers between them, resulting in a centrosymmetric space group. The alternating double and triple-layer units in $K_{2.70}Pb_{5.15}(CO_3)_5F_3$ cannot accommodate inversion centers between them, and the space group is therefore noncentrosymmetric. The rigid Pb-(CO_3)-F frameworks form large internal cavities which contain the potassium cations. In $KPb_2(CO_3)_2F$ these cavities are fully occupied. However, in $K_{2.70}Pb_{5.15}(CO_3)_5F_3$ the cavities in the double-layers are only 70% occupied by K^+, with the remaining 30% populated half the time with Pb^{2+} and half the time vacant.

The intrinsically asymmetric structures of the double and triple-layers in $KPb_2(CO_3)_2F$ and $K_{2.70}Pb_{5.15}(CO_3)_5F_3$ make a positive contribution to NCS material engineering. Understanding the crystallographic architecture of these two materials opens up the possibility of controlling the packing and polar directionality of these new structural building blocks. We intend to investigate this family of compounds further by changing alkaline metals and lone-pair cations to create other novel NCS materials.

■ ASSOCIATED CONTENT

Ⓢ Supporting Information

X-ray crystallographic file in CIF format, experimental and calculated powder X-ray diffraction patterns, Infrared and UV−vis spectra, thermogravimetric and differential thermal analysis diagrams, powder second-harmonic generation, piezoelectric loops, EDS analysis, atomic coordinates and detailed bond valence calculation tables. This material is available free of charge via the Internet at http://pubs.acs.org.

■ AUTHOR INFORMATION

Corresponding Author

*E-mail: psh@uh.edu.

Notes

The authors declare no competing financial interest.

■ ACKNOWLEDGMENTS

We would like to thank DOE-BES (DE-SC0005032) for support. We thank Prof. Angela Moeller (UH) and Dr. Dana E. Gheorghe for assistance in the IR measurements. We thank Prof. Kenneth Poeppelmeier (Northwestern University) and Martin Donakowski for assistance in UV−vis reflectance measurement, and Dr. K. Müller (UH) for assistance in quantitative EDS analysis. We also thank Prof. Craig Fennie and Dr. Jiangang He (Cornell University) for the ELF calculations and diagram.

■ REFERENCES

(1) Nalwa, H. S. *Handbook of Advanced Electronic and Photonic Materials and Devices*; Academic Press: San Diego, CA, 2001.
(2) Jona, F.; Shirane, G. *Ferroelectric Crystals*; Pergamon Press: Oxford, U.K., 1962.
(3) Auciello, O.; Scott, J. F.; Ramesh, R. *Phys. Today* **1998**, *51*, 22.
(4) Haertling, G. H. *J. Am. Ceram. Soc.* **1999**, *82*, 797.
(5) Cady, W. G. *Piezoelectricity; an Introduction to the Theory and Applications of Electromechanical Phenomena in Crystals*; Dover: New York, 1964.
(6) Jaffe, B.; Cook, W. R.; Jaffe, H. L. C. *Piezoelectric Ceramics*; R.A.N. Publishers: Marietta, OH, 1990.
(7) Munn, R. W., Ironside, C. N., Eds.; *Principles and Applications of Nonlinear Optical Materials*; CRC Press Inc.: Boca Raton, FL, 1993.
(8) Rieckhoff, K. E.; Peticolas, W. L. *Science* **1965**, *147*, 610.
(9) Donakowski, M. D.; Gautier, R.; Yeon, J.; Moore, D. T.; Nino, J. C.; Halasyamani, P. S.; Poeppelmeier, K. R. *J. Am. Chem. Soc.* **2012**, *134*, 7679.
(10) Pinlac, R. A. F.; Stern, C. L.; Poeppelmeier, K. R. *Crystals* **2011**, *1*, 3.
(11) Pinlac, R. A. F.; Marvel, M. R.; Lesage, J. J. M.; Poeppelmeier, K. R. *Mater. Res. Soc. Symp. Proc.* **2009**, *1148E*, 01−04.
(12) Pan, S.; Smit, J. P.; Marvel, M. R.; Stampler, E. S.; Haag, J. M.; Baek, J.; Halasyamani, P. S.; Poeppelmeier, K. R. *J. Solid State Chem.* **2008**, *181*, 2087.
(13) Marvel, M. R.; Pinlac, R. A. F.; Lesage, J.; Stern, C. L.; Poeppelmeier, K. R. *Z. Anorg. Allg. Chem.* **2009**, *635*, 869.
(14) Marvel, M. R.; Lesage, J.; Baek, J.; Halasyamani, P. S.; Stern, C. L.; Poeppelmeier, K. R. *J. Am. Chem. Soc.* **2007**, *129*, 13963.
(15) Halasyamani, P. S.; Poeppelmeier, K. R. *Chem. Mater.* **1998**, *10*, 2753.
(16) Hu, T.; Hu, C.-L.; Kong, F.; Mao, J.-G.; Mak, T. C. W. *Inorg. Chem.* **2012**, *51*, 8810.
(17) Mao, J.; Sun, C.; Hu, T.; Yang, B. Pacifichem 2010. *International Chemical Congress of Pacific Basin Societies*, Honolulu, HI, Dec 15−20, 2010; American Chemical Society: Washington, DC, 2010; pp INOR-558.
(18) Sun, C.-F.; Hu, C.-L.; Xu, X.; Yang, B.-P.; Mao, J.-G. *J. Am. Chem. Soc.* **2011**, *133*, 5561.
(19) Zhang, J.-H.; Hu, C.-L.; Xu, X.; Kong, F.; Mao, J.-G. *Inorg. Chem.* **2011**, *50*, 1973.
(20) Sun, C.-F.; Hu, C.-L.; Xu, X.; Ling, J.-B.; Hu, T.; Kong, F.; Long, X.-F.; Mao, J.-G. *J. Am. Chem. Soc.* **2009**, *131*, 9486.
(21) Fry, A. M.; Seibel, H. A.; Lokuhewa, I. N.; Woodward, P. M. *J. Am. Chem. Soc.* **2012**, *134*, 2621.
(22) Garcia-Martin, S.; King, G.; Urones-Garrote, E.; Nenert, G.; Woodward, P. M. *Chem. Mater.* **2011**, *23*, 163.
(23) Muller, E. A.; Cannon, R. J.; Sarjeant, A. N.; Ok, K. M.; Halasyamani, P. S.; Norquist, A. J. *Cryst. Growth Des.* **2005**, *5*, 1913.
(24) Zhang, G.; Li, Y.; Jiang, K.; Zeng, H.; Liu, T.; Chen, X.; Qin, J.; Lin, Z.; Fu, P.; Wu, Y.; Chen, C. *J. Am. Chem. Soc.* **2012**, *134*, 14818.
(25) West, J. P.; Sulejmanovic, D.; Hwu, S.-J.; He, J.; VanDerveer, D.; Johnson, B. K. *Inorg. Chem.* **2012**, *51*, 9723.
(26) Wu, H.; Pan, S.; Poeppelmeier, K. R.; Li, H.; Jia, D.; Chen, Z.; Fan, X.; Yang, Y.; Rondinelli, J. M.; Luo, H. *J. Am. Chem. Soc.* **2011**, *133*, 7786.
(27) Zhang, G.; Qin, J.; Liu, T.; Li, Y.; Wu, Y.; Chen, C. *Appl. Phys. Lett.* **2009**, *95*, 261104/1.
(28) Luo, J.; Pan, S.; Li, H.; Zhou, Z.; Yang, Z. *J. Mater. Sci.* **2011**, *46*, 7443.
(29) Wang, L.; Pan, S.; Chang, L.; Hu, J.; Yu, H. *Inorg. Chem.* **2012**, *51*, 1852.
(30) Yu, H.; Pan, S.; Wu, H.; Zhao, W.; Zhang, F.; Li, H.; Yang, Z. *J. Mater. Chem.* **2012**, *22*, 2105.
(31) Huang, H.; Yao, J.; Lin, Z.; Wang, X.; He, R.; Yao, W.; Zhai, N.; Chen, C. *Chem. Mater.* **2011**, *23*, 5457.
(32) Ren, P.; Qin, J.; Chen, C. *Inorg. Chem.* **2002**, *42*, 8.
(33) Zhang, G.; Qin, J.; Liu, T.; Zhu, T.; Fu, P.; Wu, Y.; Chen, C. *Cryst. Growth Des.* **2008**, *8*, 2946.
(34) Chang, H. Y.; Kim, S. W.; Halasyamani, P. S. *Chem. Mater.* **2010**, *22*, 3241.
(35) Yeon, J.; Kim, S.-H.; Nguyen, S. D.; Lee, H.; Halasyamani, P. S. *Inorg. Chem.* **2012**, *51*, 609.
(36) Yeon, J.; Kim, S.-H.; Nguyen, S. D.; Lee, H.; Halasyamani, P. S. *Inorg. Chem.* **2012**, *51*, 2662.
(37) Nguyen, S. D.; Kim, S.-H.; Halasyamani, P. S. *Inorg. Chem.* **2011**, *50*, 5215.
(38) Chang, H.-Y.; Kim, S.-H.; Ok, K. M.; Halasyamani, P. S. *J. Am. Chem. Soc.* **2009**, *131*, 6865.
(39) Chang, H. Y.; Sivakumar, T.; Ok, K. M.; Halasyamani, P. S. *Inorg. Chem.* **2008**, *47*, 8511.
(40) Kim, S.-H.; Yeon, J.; Halasyamani, P. S. *Chem. Mater.* **2009**, *21*, 5335.
(41) Kim, J.-H.; Halasyamani, P. S. *J. Solid State Chem.* **2008**, *181*, 2108.
(42) Yeon, J.; Kim, S.-H.; Halasyamani, P. S. *J. Solid State Chem.* **2009**, *182*, 3269.
(43) Yeon, J.; Kim, S.-H.; Halasyamani, P. S. *Inorg. Chem.* **2010**, *49*, 6986.
(44) Yeon, J.; Kim, S.-H.; Hayward, M. A.; Halasyamani, P. S. *Inorg. Chem.* **2011**, *50*, 8663.
(45) Halasyamani, P. S. *Chem. Mater.* **2004**, *16*, 3586.
(46) Opik, U.; Pryce, M. H. L. *Proc. R. Soc. London, Ser. A* **1957**, *238*, 425.
(47) Pearson, R. G. *J. Am. Chem. Soc.* **1969**, *91*, 4947.
(48) Pearson, R. G. *J. Mol. Struct.: THEOCHEM* **1983**, *12*, 25.
(49) Wheeler, R. A.; Whangbo, M. H.; Hughbanks, T.; Hoffmann, R.; Burdett, J. K.; Albright, T. A. *J. Am. Chem. Soc.* **1986**, *108*, 2222.
(50) Goodenough, J. B. *Annu. Rev. Mater. Sci.* **1998**, *28*, 1.
(51) Zou, G.; Ye, N.; Huang, L.; Lin, X. *J. Am. Chem. Soc.* **2011**, *133*, 20001.
(52) Grice, J. D.; Maisonneuve, V.; Leblanc, M. *Chem. Rev.* **2007**, *107*, 114.
(53) Ben, A. A.; Kodjikian, S.; Maisonneuve, V.; Leblanc, M. *Solid State Sci.* **2006**, *8*, 1322.
(54) Ben, A. A.; Maisonneuve, V.; Kodjikian, S.; Smiri, L. S.; Leblanc, M. *Solid State Sci.* **2002**, *4*, 503.
(55) Ben, A. A.; Maisonneuve, V.; Leblanc, M. *Solid State Sci.* **2002**, *4*, 1367.
(56) Ben, A. A.; Maisonneuve, V.; Smiri, L. S.; Leblanc, M. *Solid State Sci.* **2002**, *4*, 891.
(57) Chen, X. L.; He, M.; Xu, Y. P.; Li, H. Q.; Tu, Q. Y. *Acta Crystallogr., Sect. E: Struct. Rep. Online* **2004**, *E60*, i50.
(58) Sun, Y. P.; Huang, Q. Z.; Wu, L.; He, M.; Chen, X. L. *J. Alloys Compd.* **2006**, *417*, 13.
(59) Weil, M. *Acta Crystallogr., Sect. C: Cryst. Struct. Commun.* **2002**, *C58*, i132.
(60) Jaswal, S. S.; Sharma, T. P. *J. Phys. Chem. Solids* **1973**, *34*, 509.
(61) Kinase, W.; Tanaka, M.; Nomura, H. *J. Phys. Soc. Jpn.* **1979**, *47*, 1375.
(62) Mercier, N.; Leblanc, M.; Durand, J. *Eur. J. Solid State Inorg. Chem.* **1997**, *34*, 241.
(63) Mercier, N.; Leblanc, M. *Eur. J. Solid State Inorg. Chem.* **1994**, *31*, 423.

(64) Leblanc, M.; Mercier, N.; Attfield, J. P. *Eur. J. Solid State Inorg. Chem.* **1995**, *32*, 535.
(65) *SAINT*. 4.05 ed.; Siemens Analytical X-ray Systems Inc.: Madison, WI, 1995.
(66) Sheldrick, G. M. *SHELXS-97, Program for Solution of Crystal Structures*; University of Göttingen: Göttingen, Germany: 1997.
(67) Sheldrick, G. M. *SHELXL-97, Program for Refinement of Crystal Structures*; University of Göttingen, Göttingen, Germany, 1997.
(68) Farrugia, L. J. *J. Appl. Crystallogr.* **1999**, *32*, 837.
(69) M.Kubelka, P.; Munk, F. Z. *Tech. Phys.* **1931**, *12*, 593.
(70) Tauc, J. *Mater. Res. Bull.* **1970**, *5*, 721.
(71) Ok, K. M.; Chi, E. O.; Halasyamani, P. S. *Chem. Soc. Rev.* **2006**, *35*, 710.
(72) Kurtz, S. K.; Perry, T. T. *J. Appl. Phys.* **1968**, *39*, 3798.
(73) Momma, K.; Izumi, F. *J. Appl. Crystallogr.* **2011**, *44*, 1272.
(74) Brown, I. D.; Altermatt, D. *Acta Crystallogr., Sect. B: Struct. Sci.* **1985**, *B41*, 244.
(75) Brown, I. D. *The Chemical Bond in Inorganic Chemistry*; Oxford University Press: New York, 2002; Vol. *12*.
(76) Grice, J. D.; Van, V. J.; Gault, R. A. *Can. Mineral.* **1994**, *32*, 405.
(77) Grice, J. D.; Gault, A.; Van, V. J. *Can. Mineral.* **1997**, *35*, 181.
(78) Grice, J. D.; Chao, G. Y. *Am. Mineral.* **1997**, *82*, 1255.
(79) Fu, P.; Kong, Y.; Gong, G.; Shao, M.; Qian, J. *Kuangwu Xuebao* **1987**, *7*, 298.
(80) Yang, Z.; Pertlik, F. *Neues Jahrb. Mineral., Monatsh.* **1993**, 163.
(81) Kresse, G.; Hafner, J. *Phys. Rev. B: Condens. Matter* **1993**, *48*, 13115.
(82) Kresse, G.; Furthmüller, J. *Comput. Mater. Sci.* **1996**, *6*, 15.
(83) Perdew, J. P.; Burke, K.; Ernzerhof, M. *Phys. Rev. Lett.* **1996**, *77*, 3865.
(84) Kubel, F.; Rief, A. *Z. Kristallogr.* **2006**, *221*, 600.
(85) Velazquez, M.; Ferrier, A.; Perez, O.; Pechev, S.; Gravereau, P.; Chaminade, J.-P.; Moncorge, R. *Eur. J. Inorg. Chem.* **2006**, 4168.
(86) Donoghue, M.; Hepburn, P. H.; Ross, S. D. *Spectrochim. Acta. A* **1971**, *27*, 1065.
(87) Andersen, F. A.; Brecevic, L. *Acta Chem. Scand.* **1991**, *45*, 1018.
(88) Refat, M. S.; Elsabawy, K. M. *Bull. Mater. Sci.* **2011**, *34*, 873.
(89) Nakamoto, K. *Wiley online, l. Infrared and Raman Spectra of Inorganic and Coordination Compounds*; John Wiley: Hoboken, N.J., 2007.